# Loss of sorting nexin 27 contributes to excitatory synaptic dysfunction via modulation of glutamate receptor recycling in Down syndrome

**Xin Wang**[1,2], **Yingjun Zhao**[1,3], **Xiaofei Zhang**[1], **Hedieh Badie**[4], **Ying Zhou**[2], **Yangling Mu**[5], **Li Shen Loo**[6], **Lei Cai**[6], **Robert C. Thompson**[1], **Bo Yang**[1], **Yaomin Chen**[1], **Peter F. Johnson**[7], **Chengbiao Wu**[8], **Guojun Bu**[3], **William C. Mobley**[8], **Dongxian Zhang**[1], **Fred H. Gage**[5], **Barbara Ranscht**[4], **Yun-wu Zhang**[1,3], **Stuart A. Lipton**[1,8], **Wanjin Hong**[6,9], and **Huaxi Xu**[1,3]

[1]Degenerative Disease Research Program, Center for Neuroscience, Aging, and Stem Cell Research, Sanford-Burnham Medical Research Institute, La Jolla, CA 92037, USA

[2]Graduate School of Biomedical Sciences, Sanford-Burnham Medical Research Institute, La Jolla, CA 92037, USA

[3]Fujian Provincial Key Laboratory of Neurodegenerative Disease and Aging Research, Medical College, Xiamen University, Xiamen 361005, China

[4]Tumor Microenvironment Program, Sanford-Burnham Medical Research Institute, La Jolla, CA 92037, USA

[5]Laboratory of Genetics, the Salk Institute for Biological Studies, La Jolla, CA 92037, USA

[6]Institute of Molecular and Cell Biology, 61 Biopolis Drive, Singapore 138673, Singapore

[7]Laboratory of Cancer Prevention, Center for Cancer Research, National Cancer Institute-Frederick, NIH, Frederick, MD 21701, USA

[8]Department of Neurosciences, University of California, San Diego, 9500 Gilman Drive, La Jolla, CA 92093, USA

[9]Institute for Biomedical Research, School of Pharmaceutical Sciences, Xiamen University, Xiamen 361005, China

## Abstract

Sorting nexin 27 (SNX27), a brain-enriched PDZ domain protein, regulates endocytic sorting and trafficking. Here, we show that *Snx27*^{-/-} mice exhibit severe neuronal deficits in the hippocampus and cortex. While *Snx27*^{+/-} mice exhibit grossly normal neuroanatomy, we find defects in synaptic function, learning and memory, and a reduction in ionotropic glutamate receptors (NMDARs and AMPARs). SNX27 interacts with these receptors through its PDZ domain, regulating their recycling to the plasma membrane. We demonstrate a concomitant reduction of SNX27 and C/EBPβ in Down syndrome brains and identify C/EBPβ as a transcription factor for *SNX27*. Down syndrome causes over-expression of miR-155, a chromosome 21-encoded microRNA that negatively regulates C/EBPβ, thereby reducing SNX27 and resulting in synaptic dysfunction. Up-regulating SNX27 in the hippocampus of Down syndrome mice rescues synaptic and cognitive deficits. Our identification of the role of SNX27 in synaptic function establishes a novel molecular mechanism of Down syndrome pathogenesis.

## INTRODUCTION

Sorting nexins (SNXs) are a large group of proteins that contain a conserved PX (or phagocyte oxidase homology) domain targeting SNX proteins to endosomes[1]. SNX27 was originally identified in rats as an alternative splicing product of the *Mrt1* (methamphetamine responsive transcript 1) gene[2]. SNX27 contains a PDZ (PSD-95/Disc-large/ZO-1) domain, making it unique among the PX domain proteins. PDZ domains are protein-protein interaction domains often found in the postsynaptic density (PSD) of neuronal excitatory synapses.

SNX27 reportedly participates in the dynamic trafficking of receptors and ion channels such as β2-adrenergic receptors (β2-AR)[3,4], G-protein-activated inward rectifying potassium type 2 (GIRK2)[5], serotonin receptor subunit 4a (5-HT4a)[6] and *N*-Methyl-D-aspartate (NMDA)– type glutamate receptor subunit 2C (NR2C)[7]. However, the physiological role of SNX27 at synapses and whether SNX27 regulates the trafficking of other major types of glutamate receptors remains unknown.

In the PSDs of excitatory synapses, different classes of glutamate receptors are responsible for transducing the presynaptic signal into both biochemical and electrical events in the postsynaptic neuron. The two major types of glutamate receptors are α-Amino-3-hydroxy-5-methyl-4-isoxazolepropionic acid (AMPA)–type glutamate receptors (AMPARs) and NMDA receptors (NMDARs). Dysregulation of AMPARs and NMDARs are involved in several neurodegenerative diseases[8,9].

Down syndrome, or trisomy 21, is a congenital disorder that manifests as defects in multiple organs and causes developmental delays and learning disabilities. People with Down syndrome have an extra copy of chromosome 21, leading to an over-dosage of the gene products and non-coding RNAs encoded by this chromosome. Down syndrome pathology includes neuropathology of the cortex and hippocampus in both developmental and aging processes. Dramatic dendritic and synaptic abnormalities, including decreased dendritic arborization[10] and a reduction in synaptic number, have been observed in both prenatal[11,12]

and postnatal Down syndrome brains[13]. The balance between excitatory and inhibitory synapses is reportedly impaired in the brains of both humans with Down syndrome and mouse models[14,15]. Impaired LTP has also been detected in the hippocampal CA1 region of Ts65Dn mice[16,17]. Although several chromosome 21-encoded products, such as β-amyloid precursor protein (APP), are thought to contribute to the pathology of Down syndrome, the detailed molecular mechanisms remain largely unclear.

Here, we demonstrate a novel role for SNX27 in the dysregulation of synaptic function in Down syndrome. Our study shows that the chromosome 21-encoded miR-155 targets and down-regulates C/EBPβ, which is a transcription factor for *SNX27*. Thus, the lower levels of C/EBPβ in Down syndrome lead to reduced SNX27 expression. We show that SNX27 promotes recycling of AMPARs and NMDARs from early endosomes to the plasma membrane through direct PDZ binding and thus prevents their degradation. Deletion of *SNX27* in mice results in synaptic dysfunctions and cognitive deficits. Further, over-expressing SNX27 in the hippocampus of Ts65Dn mice reverses the impairments in the receptor levels and synaptic functions. Therefore, SNX27 is crucial for maintaining glutamate receptors via posttranslational mechanisms and is required for normal synaptic activity and long-term memory formation.

## RESULTS

### Neuropathology in the cortex and hippocampus of *Snx27⁻/⁻* mice

We first examined the developmental expression pattern of Snx27 in postnatal mouse brains and found that Snx27 can be detected at P0 and reaches a plateau at P7. The developmental expression pattern of Snx27 is similar to that of GluR1 and NR1 (Fig. 1a). In situ hybridization results, as reported by the Allen Brain Atlas, revealed that Snx27 mRNA is highly expressed in the cortex, hippocampus and cerebellum (Supplementary Fig. 1). To investigate the physiological function of SNX27, we analyzed *Snx27* knockout mice and found that most *Snx27⁻/⁻* mice are viable from birth until postnatal day 14 (P14). Their growth rate then slowed significantly and mice die by week 4. Microscopic histological examination of *Snx27⁻/⁻* brains revealed degenerating neurons in the cortex at P14, with reduced somal size and hyperchromicity apparent (Fig. 1b).

Brain development during the early postnatal period involves increases in dendritic branching and synapse formation, both of which were found to be greatly compromised in *Snx27⁻/⁻* mice at P14 (Fig. 1c,d). Although the orientation of apical dendrites is unaffected, the total dendritic length of both cortical layer 5 and hippocampal CA1 neurons is dramatically reduced. There is also a marked decrease in dendritic branching in cortical neurons.

### Impaired learning and memory in *Snx27⁺/⁻* mice

Complete loss of *Snx27* results in severe neuronal death and eventual lethality in mice, making it impossible to determine how Snx27 influences memory deficits and synaptic function. However, *Snx27⁺/⁻* mice are viable and exhibit grossly normal neuroanatomy

(Supplementary Fig. 2) and lifespan[7] compared to $Snx27^{+/+}$ littermates; thus, we examined the role of Snx27 in memory and synaptic function using $Snx27^{+/-}$ mice.

Since intellectual disability is a primary aspect of Down syndrome, we assessed potential cognitive deficits in $Snx27^{+/-}$ mice using behavioral tests. We first used the Barnes maze[18,19] to assess learning and memory and found that $Snx27^{+/-}$ mice made more errors at day 6–8 after training (Fig. 2a) and used less spatial strategies than $Snx27^{+/+}$ mice (Supplementary Fig. 3a). $Snx27^{+/-}$ mice did not spend significantly more time in the target quadrant than other quadrants in the probe test (Fig. 2b). Furthermore, $Snx27^{+/-}$ mice spent much less time exploring novel objects than familiar objects in the novel object recognition task compared to $Snx27^{+/+}$ mice (Fig. 2c). We performed additional behavioral tasks to test for locomotor activity (Supplementary Fig. 3b–d) or visual disabilities (Supplementary Fig. 4a) and found no differences between $Snx27^{+/+}$ and $Snx27^{+/-}$ mice.

## Impaired synaptic transmission and synaptic plasticity in $Snx27^{+/-}$ mice

We performed extracellular recordings on hippocampal slices to examine LTP in the hippocampal CA1 region. Input–output response results showed that $Snx27^{+/-}$ mice have decreased excitatory synaptic transmission compared to $Snx27^{+/+}$ mice (Fig. 2e). The attenuation of basal synaptic transmission in $Snx27^{+/-}$ mice may arise from a reduced number of synapses or defects in either presynaptic or postsynaptic function. To distinguish between these possibilities, we used a paired-pulse facilitation (PPF) paradigm to examine the regulation of synaptic activity through $Ca^{2+}$-mediated presynaptic neurotransmitter release. We found that the PPF ratio was unchanged in $Snx27^{+/-}$ brain slices compared to $Snx27^{+/+}$ controls (Fig. 2f). In contrast, when we recorded miniature excitatory postsynaptic currents (mEPSCs) from CA1 hippocampal neurons, the amplitude was significantly decreased in $Snx27^{+/-}$ neurons compared to $Snx27^{+/+}$ neurons, while the frequency remained unaltered (Fig. 2g–i).

Given the defect is postsynaptic, we reasoned that synaptic plasticity should also be disrupted. In fact, when we examined NMDAR-dependent synaptic plasticity in $Snx27^{+/-}$ mice, we found that long-term potentiation (LTP) induced by high frequency trains (100 Hz for 1 s) was decreased compared to $Snx27^{+/+}$ controls (Fig. 2i). Since, in addition to input-output curves, the mEPSCs data represent AMPAR-mediated responses, and the induction of LTP is dependent upon intact NMDAR activity, our electrophysiological data suggest that $Snx27^{+/-}$ mice possess defects in both AMPAR and NMDAR-dependent synaptic events.

## Reduced levels of hippocampal glutamate receptors in $Snx27^{+/-}$ mice

We determined through Western blot analysis that $Snx27^{+/-}$ mice had lower levels of GluR1, GluR2, NR1, NR2A and NR2B in both synaptosomal membranes and PSD fractions compared to $Snx27^{+/+}$ littermates (Fig. 3a). We examined the total levels of glutamate receptor subunits in the hippocampus and observed at P1 that the levels of GluR1, GluR2 and NR1, but not NR2A and NR2B, were decreased in $Snx27^{-/-}$ mice compared to $Snx27^{+/+}$ mice. However, by P14, the levels of NR2A and NR2B were also decreased (Supplementary Fig. 5). PSD-95 levels were unaffected at both time points.

### Loss of SNX27 results in increased degradation of AMPARs and NMDARs

We performed quantitative RT-PCR to measure receptor mRNA levels and found them unaffected in the hippocampi of $Snx27^{-/-}$ mice compared to littermate controls (Supplementary Fig. 6). To determine whether SNX27 influences turnover of the receptors, we performed cycloheximide chase assays in HEK293 cells over-expressing GluR1 (GluR1-HEK293) or NR1(NR1-HEK293). The turnover of both GluR1 and NR1 were significantly accelerated by the siRNA down-regulation of SNX27 (Fig. 3b,c). Treatment of GluR1-HEK293 or NR1-HEK293 cells with the proteasomal inhibitor lactacystin or MG132 in the presence of cycloheximide largely rescued the degradation of GluR1 and NR1 caused by SNX27 knockdown. Treatment with the lysosomal inhibitor leupeptin or $NH_4Cl$ also rescued, although to a lesser extent, receptor degradation (Fig. 3d,e).

### SNX27 interacts with glutamate receptors and regulates their recycling to the cell surface

We found that both a recombinant SNX27 PDZ domain and full length SNX27 protein linked with GST can pull down glutamate receptors (GluR1, GluR2, NR1 and NR2A) but not the presynaptic vesicle protein synaptophysin from mouse brain lysates (Fig. 4a). Myc-tagged SNX27 and constructs expressing various glutamate receptors were co-transfected into HEK293T cells and their interaction was verified by co-immunoprecipitation (Fig. 4b). Moreover, endogenous Snx27 co-immunoprecipitated with endogenous glutamate receptors from mouse brain lysates (Fig. 4c).

Cell surface biotinylation experiments showed that over-expression of SNX27 resulted in increased cell surface levels of GluR1 and NR1 (Fig. 4d). Conversely, knockdown of SNX27 resulted in reduced cell surface levels of GluR1 and NR1 (Fig. 4e). This effect was also evident in primary neurons; we observed a decrease in cell surface levels of GluR1 and NR1 in primary neurons derived from $Snx27^{+/-}$ mice (Fig. 4f).

The steady state level of cell surface receptors is the net result of both endocytosis and recycling of the receptors. Since SNX27 did not influence the endocytosis of GluR1 (Supplementary Fig. 7), we postulated that SNX27 affects the recycling of the receptors. To test this hypothesis, we carried out receptor recycling assays and found that over-expression of SNX27 decreased levels of internalized biotinylated GluR1, indicating an accelerated recycling rate (Fig. 4g). Consistent with these over-expression experiments, we found slower recycling of biotin-labeled GluR1 upon treatment with SNX27 siRNA, as compared to controls (Fig. 4h).

### Reduction of SNX27 expression in Down syndrome brains

We examined the levels of SNX27 in brain samples from humans with Down syndrome and age/gender matched controls and found both protein and mRNA levels of SNX27 were markedly decreased in the cortex of Down syndrome individuals (Fig. 5a,c). Consistent with changes in SNX27, the levels of GluR1 were also decreased in Down syndrome brains while APP levels were significantly increased, as expected. However, the levels of SNX27 were not altered in the cortexes of humans with sporadic Alzheimer's disease compared to controls (Fig. 5b). We also found, as expected, that both Snx27 and C/EBPβ protein levels were lower in the hippocampus of Ts65Dn mice than in wild-type (WT) controls

(Supplementary Fig. 8a). However, only Snx27, and not C/EBPβ, mRNA levels were reduced in the hippocampus of Ts65Dn mice (Supplementary Fig. 8b).

## Regulation of SNX27 by the miR-155—C/EBPβ pathway

We next examined the expression levels of chromosome 21-derived microRNAs in Down syndrome cortexes. Our findings were consistent with previous studies demonstrating increased levels of chromosome 21-encoded microRNAs in the brains of both humans with Down syndrome and Ts65Dn mice[20,21] (Supplementary Fig. 9a and Supplementary Fig. 8c). Among these microRNAs, only miR-155 expression is negatively correlated with SNX27 mRNA levels (Supplementary Fig. 9b). We transfected a miR-155 mimic into human neuroblastoma MC-IXC cells and found decreased levels of both SNX27 protein and mRNA (Fig. 5d,e). However, no consensus miR-155 binding sites were found on the SNX27 3′-UTR, suggesting that SNX27 is not the direct target. In silico analysis predicted several C/EBPβ binding sites in the SNX27 promoter region (Supplementary Fig. 10), and the binding of miR-155 to the C/EBPβ 3′-UTR was recently reported[22]. Additionally, we observed a positive correlation between C/EBPβ and SNX27 protein levels in the cerebrocortex of humans with Down syndrome (Supplementary Fig. 9c).

We over-expressed an active isoform of C/EBPβ, LAP2 (Liver-enriched activator protein), in MC-IXC human neuroblastoma cells and found that SNX27 protein levels were significantly up-regulated (Fig. 5f). Moreover, we determined that Snx27 protein levels were decreased in the cortex and hippocampi of *Cebpb*^{−/−} mice compared to *Cebpb*^{+/−} controls (Fig. 5g). A Luciferase reporter assay using Hela cells showed that over-expression of LAP2 enhanced the promoter activity of human *SNX27*, whereas over-expression of another C/EBPβ isoform, LIP (Liver inhibitory protein), did not affect *SNX27* promoter activity (Fig. 5h). We carried out a chromatin immunoprecipitation (ChIP) assay and found that C/EBPβ binds to the endogenous *SNX27* promoter in HEK293T cells (Fig. 5i).

## Over-expression of SNX27 rescues impaired synaptic functions in Ts65Dn mice

To test whether SNX27 expression could rescue the synaptic deficits and impaired learning and memory of Down syndrome, we generated Adeno-associated viruses (AAV1) containing human *SNX27* cDNA (Fig. 6a). As expected, over-expression of human SNX27 increased levels of GluR1, GluR2, NR1, NR2A and NR2B in rat primary neurons (Supplementary Fig. 11). We next injected the AAV-SNX27 or AAV-GFP control bilaterally into the hippocampal CA1 area of 7~8 month old Ts65Dn or WT mice and analyzed subsequent behavioral changes (Fig. 6c). Four weeks after injection of AAV-SNX27, SNX27 levels in Ts65Dn mice were significantly higher than in controls (Fig. 6f). Since CA1-specific deletion of NMDAR1 can result in impaired performance on novel object recognition tests[23], and Ts65Dn mice exhibit impaired LTP and novel object recognition memory[24], this test may allow us to evaluate hippocampus-dependent memory. Notably, the cognitive and LTP deficits in Ts65Dn mice[16,24] were rescued by increased SNX27 expression (Fig. 6b–e). All mice behaved normally on the optomotor test (Supplementary Fig. 4b), excluding the possible confounding effects of visual problems (a small portion of Ts65Dn mice may become blind[25]). In synaptosomal preparations from Ts65Dn mice, the levels of glutamate receptor subunits GluR1, NR1 and NR2B were lower

than in control mice (Supplementary Fig. 9d). Reduced levels of synaptosomal glutamate receptors were rescued by exogenous expression of SNX27 in the hippocampi of the Ts65Dn mice (Fig. 6f).

## DISCUSSION

### DS-like neuronal deficits in *Snx27⁻/⁻* mice

Dramatic dendritic and synaptic abnormalities such as decreased dendritic arborization and reduced synapse numbers in both prenatal and postnatal Down syndrome brains have been reported[13]. Similarly, dendritic growth and branching is greatly compromised in *Snx27⁻/⁻* mice analyzed at early postnatal stages. The decreased dendritic branching and synapse number suggest that *Snx27* is essential for postnatal brain development.

Abnormalities in excitatory neurotransmission and cognitive function have been reported in humans with Down syndrome as well as in mouse models[14,15,26]. Decreased LTP has been observed in both Ts65Dn and Tc1 Down syndrome mouse models[16,17,26]. To investigate whether *Snx27* deficiency results in synaptic and cognitive deficits, we used *Snx27⁺/⁻* mice for electrophysiological and behavioral studies, as *Snx27⁻/⁻* mice show severe neuropathology and early lethality. Additionally, the *Snx27⁺/⁻* mouse model might better mimic the pathology of human Down syndrome, which is due to only a partial loss of SNX27 expression.

mEPSC recordings reveal that AMPAR-mediated postsynaptic currents are reduced in the hippocampi of *Snx27⁺/⁻* mice compared to controls. Furthermore, NMDAR-dependent Schaffer-collateral CA1 LTP induction is significantly attenuated in *Snx27⁺/⁻* mice, indicating a possible role for Snx27 in the LTP mechanism.

### SNX27 mediates glutamate receptor recycling

The balance between insertion and internalization of AMPARs at the postsynaptic membrane is an important mechanism for regulating synaptic strength. Our biochemical and cell biological data show that SNX27 promotes NMDAR and AMPAR recycling back to the plasma membrane and is not involved in the internalization of these receptors.

In the future, it will be interesting to study whether SNX27 regulates the recycling of NMDARs and AMPARs in cooperation with other components of the trafficking machinery. For example, SNX27, like SNX17, contains a C-terminal PX-FERM domain and reportedly the FERM domain can associate with the activated Ras small GTPase[27]. It is still unclear, however, if SNX27 interacts with the small GTPase to regulate the sorting and recycling of NMDARs and AMPARs. Additionally, the retromer has also been shown to regulate the transport of various cargo from the endosome to the Trans-Golgi Network (TGN) and plasma membrane directly. Previous studies showed cooperation between SNX27 and the retromer complex in regulation of β2-AR recycling[4]. Mutation and dysfunction of the retromer complex have been linked with neurodegenerative diseases, including Alzheimer's disease[28–31] and Parkinson's disease (PD)[32,33], further investigation on whether SNX27 regulates recycling of AMPARs and NMDARs in a retromer-dependent manner will be interesting.

### A miR-155—C/EBPβ—SNX27 pathway in Down syndrome pathogenesis

miR-155, encoded on chromosome 21 and thus over-expressed in Down syndrome, is a negative regulator of C/EBPβ[22]. Previous studies have suggested that C/EBP is crucial for consolidation of long-term memory in both invertebrates and mice[34–37]. C/EBPβ is an evolutionarily conserved gene with a selective role in the consolidation of new memories in the hippocampus. Our results indicate that SNX27, a downstream target of C/EBPβ, is down-regulated in Down syndrome brains. Notably, restoration of SNX27 by AAV site-specific delivery reverses the LTP and cognitive deficits of Ts65Dn mice. Loss of SNX27 may partially explain the mechanism whereby Trisomy 21 leads to synaptic dysfunction, memory difficulties and neurodegeneration.

We found nearly normal protein expression levels of GABA$_A$ receptor subunits (α1, β2) in the hippocampus of $Snx27^{+/-}$ mice. We also determined, using co-immunoprecipitation, that SNX27 does not interact with GABA$_A$ receptor subunits (α1, β2) (Supplementary Fig. 12). These results suggest that SNX27 does not affect GABA$_A$ receptors. However, previous studies have reported that SNX27 negatively regulates GIRK2[5], which is encoded by chromosome 21 and highly expressed in Down syndrome brains. Since GIRK2 controls the excitability of neurons through GIRK-mediated self-inhibition, its over-expression is involved in the excessive inhibition in Down syndrome brains[38,39]. Therefore, SNX27 expression could contribute to the restoration of balance between excitation and inhibition through both up-regulation of excitatory transmission and suppression of GIRK2-mediated inhibition.

In summary, we have identified a signaling pathway in which the decreased C/EBPβ level resulting from excessive miR-155 in Down syndrome, represses SNX27 expression (Supplementary Fig. 13). This leads to synaptic dysfunction and neuropathological changes. Thus, the miR-155—C/EBPβ—SNX27 pathway is a novel contributory mechanism to the neuropathogenesis of Down syndrome.

## ONLINE METHODS

### Antibodies

The SNX27 antibodies used in these experiments include the previously described SNX27 polyclonal antibodies and SNX27 monoclonal antibodies[7,40]. Other antibodies acquired from commercial sources were: GluR1 (Chemicon), GluR2 (Millipore), PSD-95 (Millipore), synaptophysin (Sigma), NR1 (BD Biosciences), NR2A (Millipore), NR2B (BD Biosciences), VGAT (Millopore), GABA$_A$Rα1 (Millipore), GABA$_A$Rβ2 (Millipore), C/EBPβ (Santa Cruz), Transferrin receptor (Invitrogen), c-Myc (Invitrogen), α-tubulin (Sigma) and β-actin (Sigma).

### Constructs

The following vectors were used in this study: pCI-neo (Promega), pDMyc-SNX27, GluR1 and GluR2, NR1 and NR2A, and pDMyc-Neo and pDHA-Neo (Modified from pCI-neo). Both Full-length and PDZ domain sequences of *SNX27* were amplified by PCR and then inserted into pGEX-4T2 (GE Healthcare) for GST pull down assays. GluR1 and GluR2

constructs were from Paul Greengard's lab. Constructs expressing LAP2 and LIP (Addgene plasmid 15738 and 12561) were ordered from Addgene and described in the previous study[41].

## Mouse strains

*Snx27*^{+/+}, *Snx27*^{+/−} and *Snx27*^{−/−} mice[7] were generated by crossing heterozygotes on C57Bl/6 and 129SV mixed backgrounds to produce F1 hybrid background animals.

*Cebpb*^{+/−} and *Cebpb*^{−/−} mice[42] were generated by crossing heterozygotes on C57Bl/6 and 129SV backgrounds to produce F1 hybrid background animals.

Segmental trisomy 16 (Ts65Dn) mice were obtained by mating female carriers of the 17[16] chromosome (B6EiC3H-a/A-Ts65Dn) with (C57BL/6JEi X C3H/HeJ) F1 (JAX #JR1875) males[25]. Ts65Dn mice were maintained on the B6/C3H background. Diploid (2N) littermate mice served as WT controls. All mice were also screened for retinal degeneration due to Pde6brd1 homozygosity and only animals free of retinal degeneration were used for behavioral tests.

All procedures involving animals were performed under the guidelines of Sanford-Burnham Medical Research Institute (SBMRI) Institutional Animal Care and Use Committee.

## Preparation of synaptosomal and PSD fractions from mouse hippocampus

Mouse hippocampi were dissected and homogenized on ice in 10 volumes of cold sucrose buffer (0.32M Sucrose, 25mM HEPES pH=7.4). The homogenates were centrifuged at 300g for 5 min to separate supernatant (S1) from the nuclei and large debris fraction. The S1 fraction was centrifuged at 10,000g for 12 min to separate the supernatant (S2: light membrane and cytosolic fraction) and the pellet (P2: crude synaptosomal fraction). The P2 fraction was washed twice by sucrose buffer and resuspended in cold HBS buffer (25mM HEPES pH=7.4, 150mM NaCl) to get the synaptosomal fraction. The PSD fraction was prepared by solubilizing the synaptosomal fraction in 1% Triton HBS buffer at 4 °C for 30 min, then centrifuging at 10,000g for 20 min.

## siRNA, miRNA mimic and quantitative Real-Time PCR

The human SNX27 siRNA used was: 5′-CCAGAUGGAACAACGGUUATT-3′. The control siRNA was from QIAGEN. The miRIDIAN miR-155 mimic was from Dharmacon. siRNA or miRNA was transfected into HEK293T or MC-IXC cells using Lipofectamine RNAiMAX. The real-time PCR primer sequence is in Supplementary Table 3. β-actin served as the control. Relative microRNA expression was determined using real-time quantitative PCR and normalized to U6 expression as an internal control. Total RNA was isolated using Trizol Reagent (Invitrogen) and 500ng of total RNA was reverse transcribed using microRNA First-Strand Synthesis and Quantitation Kits (Clontech).

## GST pull-down assays

Full-length (FL) SNX27 and SNX27 PDZ domain cDNAs were cloned into the pGEX4T1 vector. Glutathione S-transferase (GST)-fused recombinant proteins were purified as

described previously[7]. We performed GST pull-down assays in the binding buffer (20 mM Tris-HCl, pH 8.0, 100 mM NaCl, 1 mM EDTA, 1% NP-40, supplemented with protease inhibitors). After washing, retained proteins were eluted by boiling in SDS protein loading buffer and analyzed by Western blot using the indicated antibodies.

### Immunoprecipitation

293T cells transfected with different expression constructs were lysed in NP-40 buffer (20 mM Tris-HCl, pH 8.0, 100 mM NaCl, 1 mM EDTA, 1% NP-40, supplemented with protease inhibitors). Lysates were immunoprecipitated using mouse IgG, rabbit IgG, and antibodies against Myc or HA and Trueblot IP beads (eBioscience), followed by Western blot.

### Promoter luciferase assay

Briefly, the human *SNX27* promoter was amplified using genomic DNA from 293T cells as templates. After amplification, PCR products were inserted into the pGL3-Basic vector containing the firefly luciferase gene (Promega). Firefly luciferase vectors were cotransfected with phRL-SV40 containing the Renilla luciferase gene (Promega) into Hela cells with altered C/EBPβ (over-expressed or down-regulated) for 48 h. Firefly luciferase activities were assayed and normalized to those of Renilla luciferase.

### Chromatin immunoprecipitation

ChIP assays were performed with a commercial kit (Upstate) following the manufacturer's instructions with minor modifications. *SNX27* promoter primers are shown in Supplementary Table 3. PCR products were resolved on 2% agarose gels and visualized after ethidium bromide staining.

### Pharmacological treatment of cycloheximide, proteasomal and lysosomal inhibitors

Cells were incubated for 8 hours with cycloheximide (CHX, 500 μM), in the presence or absence of lysosomal inhibitor (100 μg ml$^{-1}$ leupeptin, 50mM NH$_4$Cl, Sigma) or proteasomal inhibitor (10 μM MG132 and 10 μM lactacystin from Calbiochem). After treatment, cells were lysed and subjected to western blot analysis.

### Immunohistochemistry and data analyses

*Snx27*$^{-/-}$ or *Snx27*$^{+/-}$ mice and *Snx27*$^{+/+}$ littermate controls were anesthetized and fixed by cardiac perfusion with 4% PFA. Whole brains were excised and post-fixed in 4% PFA overnight. Tissue blocks were embedded in paraffin and 5μm sections were cut and stained with Nissl (cresyl violet). Immunostained sections were examined and fluorescence images collected using a Zeiss fluorescence microscope with AxioVision software.

### Golgi staining

Golgi staining was performed by using the FD Rapid GolgiStain Kit (FD NeuroTechonologies). Images were acquired using a Zeiss fluorescence microscope with a 10× or 20× objective under DIC. Dendritic branching and length were measured using NIH

Image J-software with a previously described sholl analysis plug-in[43]. Student's t test was used to determine the significance between $Snx27^{+/+}$ and $Snx27^{-/-}$ neurons.

### Cell surface biotinylation assay

Biotinylation was carried out following a previously described protocol[44].

### Receptor recycling experiments

Receptor recycling experiments were performed as described[45]. Briefly, cells were specifically labeled with Sulfo-NHS-SS-biotin at 4 °C. After washing, cells were incubated at 37 °C for 30 min to allow endocytosis to occur. Cells were then cooled to 4 °C to stop membrane trafficking and biotin was cleaved from biotinylated proteins remaining at the cell surface with glutathione. Cells were then incubated with serum-free growth media containing 50 mM glutathione at 37 °C for various times to allow internalized receptors to recycle before the cells were cooled to 4 °C again. Cells were then incubated with glutathione cleavage buffer (twice, 15 min each at 4 °C) to ensure complete cleavage of any newly appearing surface biotin. Residual biotinylated (internalized) receptors were pulled down from cell lysates by streptavidin precipitation, detected by Western blot analysis with GluR1-specific and β-actin-specific antibodies and then quantified by densitometry. The rate of reduction of biotinylated AMPARs provides a measure of the receptor recycling rate.

### Stereotactic injection of adeno-associated virus

Recombinant human SNX27 and GFP adeno-associated virus (2 μl, titer $3 \times 10^{12}$) were stereotactically injected into the hippocampus of Ts65Dn or WT mice (7~8 months old) at the following coordinates: anterior posterior, 1.8; medial lateral, ±1.8; dorsal ventral, 1.8. To confirm region-specific over-expression of SNX27 in mouse brains, 4 weeks after injection mice were anesthetized and sacrificed, whereupon brain tissues were rapidly removed. Hippocampal lysates were prepared by homogenizing tissue in RIPA buffer, in the absence of protease inhibitors, for Western blotting analysis.

### Miniature EPSC recordings

For hippocampal slice recordings, horizontal slices were prepared from $Snx27^{+/-}$ and $Snx27^{+/+}$ mice at 4 to 5 weeks of age. We performed electrophysiological recordings on transverse hippocampal slices (350 μm-thickness); 200 consecutive events were analyzed from cells of either $Snx27^{+/-}$ or $Snx27^{+/+}$ mice. See details in Supplementary Methods online.

### Extracellular electrophysiology

The acute hippocampal slices were obtained and maintained as described above. The Schaffer collateral inputs to the CA1 region were stimulated with a bipolar tungsten electrical stimulating electrode at three different intensities (min, half-max. and max.). Using a low resistance recording electrode, the field Excitatory Postsynaptic potential (fEPSP) responses from the stratum radiatum region of CA1 were recorded using a MultiClamp (Axon Instrument). The initial slope of the fEPSP response was measured using Clampex

software. Synaptic transmission of CA1 neurons was determined as input-ouput curves for fEPSP slope response to Schaffer collateral stimulation.

### Neurobehavioral tests

See Supplementary Methods online.

### Human brain specimens

Human Down syndrome brain cortex samples were obtained from the Brain and Tissue Bank for Developmental Disorders, University of Maryland at Baltimore, in contract with the National Institutes of Health, NICHD. Additional human Alzheimer's disease brain samples used in this project were provided by UCSD, San Diego, CA and were analyzed with institutional permission under California and National Institutes of Health guidelines. For specimen information see Supplementary Table 1, 2.

### Statistical analyses

Statistical analyses were performed with GraphPad Prism. Data distribution was assessed by a Kolmogorov-Smirnoff nonparametric test of equality. Differences between two means were assessed by paired or unpaired $t$ test. Differences among multiple means were assessed, as indicated, by one-way, two-way or repeated-measures ANOVA, followed by Bonferroni's, Dunnett's, Kruskal-Wallis's or Tukey's post-hoc test. Error bars represent s.e.m. Null hypotheses were rejected at the 0.05 level.

### Additional methods

Detailed methodology is described in the Supplementary Methods.

## Supplementary Material

Refer to Web version on PubMed Central for supplementary material.

## Acknowledgments

## References

1. Cullen PJ. Endosomal sorting and signalling: an emerging role for sorting nexins. Nat Rev Mol Cell Biol. 2008; 9:574–582. [PubMed: 18523436]

2. Kajii Y, et al. A developmentally regulated and psychostimulant-inducible novel rat gene mrt1 encoding PDZ-PX proteins isolated in the neocortex. Mol Psychiatry. 2003; 8:434–444. [PubMed: 12740601]

3. Lauffer BE, et al. SNX27 mediates PDZ-directed sorting from endosomes to the plasma membrane. J Cell Biol. 2010; 190:565–574. [PubMed: 20733053]

4. Temkin P, et al. SNX27 mediates retromer tubule entry and endosome-to-plasma membrane trafficking of signalling receptors. Nat Cell Biol. 2011; 13:715–721. [PubMed: 21602791]

5. Lunn ML, et al. A unique sorting nexin regulates trafficking of potassium channels via a PDZ domain interaction. Nature neuroscience. 2007; 10:1249–1259. [PubMed: 17828261]

6. Joubert L, et al. New sorting nexin (SNX27) and NHERF specifically interact with the 5-HT4a receptor splice variant: roles in receptor targeting. J Cell Sci. 2004; 117:5367–5379. [PubMed: 15466885]

7. Cai L, Loo LS, Atlashkin V, Hanson BJ, Hong W. Deficiency of sorting nexin 27 (SNX27) leads to growth retardation and elevated levels of N-methyl-D-aspartate receptor 2C (NR2C). Mol Cell Biol. 2011; 31:1734–1747. [PubMed: 21300787]

8. Shepherd JD, Huganir RL. The cell biology of synaptic plasticity: AMPA receptor trafficking. Annu Rev Cell Dev Biol. 2007; 23:613–643. [PubMed: 17506699]

9. Malinow R. New developments on the role of NMDA receptors in Alzheimer's disease. Curr Opin Neurobiol. 2011

10. Becker LE, Armstrong DL, Chan F. Dendritic atrophy in children with Down's syndrome. Ann Neurol. 1986; 20:520–526. [PubMed: 2947535]

11. Weitzdoerfer R, Dierssen M, Fountoulakis M, Lubec G. Fetal life in Down syndrome starts with normal neuronal density but impaired dendritic spines and synaptosomal structure. J Neural Transm Suppl. 2001:59–70. [PubMed: 11771761]

12. Petit TL, LeBoutillier JC, Alfano DP, Becker LE. Synaptic development in the human fetus: a morphometric analysis of normal and Down's syndrome neocortex. Exp Neurol. 1984; 83:13–23. [PubMed: 6228436]

13. Schmidt-Sidor B, Wisniewski KE, Shepard TH, Sersen EA. Brain growth in Down syndrome subjects 15 to 22 weeks of gestational age and birth to 60 months. Clin Neuropathol. 1990; 9:181–190. [PubMed: 2146054]

14. Reynolds GP, Warner CE. Amino acid neurotransmitter deficits in adult Down's syndrome brain tissue. Neurosci Lett. 1988; 94:224–227. [PubMed: 2907377]

15. Risser D, Lubec G, Cairns N, Herrera-Marschitz M. Excitatory amino acids and monoamines in parahippocampal gyrus and frontal cortical pole of adults with Down syndrome. Life Sci. 1997; 60:1231–1237. [PubMed: 9096240]

16. Siarey RJ, Stoll J, Rapoport SI, Galdzicki Z. Altered long-term potentiation in the young and old Ts65Dn mouse, a model for Down syndrome. Neuropharmacology. 1997; 36:1549–1554. [PubMed: 9517425]

17. Galdzicki Z, Siarey R, Pearce R, Stoll J, Rapoport SI. On the cause of mental retardation in Down syndrome: extrapolation from full and segmental trisomy 16 mouse models. Brain Res Brain Res Rev. 2001; 35:115–145. [PubMed: 11336779]

18. Barnes CA. Memory deficits associated with senescence: a neurophysiological and behavioral study in the rat. J Comp Physiol Psychol. 1979; 93:74–104. [PubMed: 221551]

19. Bach ME, Hawkins RD, Osman M, Kandel ER, Mayford M. Impairment of spatial but not contextual memory in CaMKII mutant mice with a selective loss of hippocampal LTP in the range of the theta frequency. Cell. 1995; 81:905–915. [PubMed: 7781067]

20. Kuhn DE, et al. Human chromosome 21-derived miRNAs are overexpressed in Down syndrome brains and hearts. Biochem Biophys Res Commun. 2008; 370:473–477. [PubMed: 18387358]

21. Keck-Wherley J, et al. Abnormal microRNA expression in Ts65Dn hippocampus and whole blood: contributions to Down syndrome phenotypes. Dev Neurosci. 2011; 33:451–467. [PubMed: 22042248]

22. He M, Xu Z, Ding T, Kuang DM, Zheng L. MicroRNA-155 regulates inflammatory cytokine production in tumor-associated macrophages via targeting C/EBPbeta. Cell Mol Immunol. 2009; 6:343–352. [PubMed: 19887047]

23. Rampon C, et al. Enrichment induces structural changes and recovery from nonspatial memory deficits in CA1 NMDAR1-knockout mice. Nature neuroscience. 2000; 3:238–244. [PubMed: 10700255]

24. Fernandez F, et al. Pharmacotherapy for cognitive impairment in a mouse model of Down syndrome. Nature neuroscience. 2007; 10:411–413. [PubMed: 17322876]

25. Davisson MT, et al. Segmental trisomy as a mouse model for Down syndrome. Prog Clin Biol Res. 1993; 384:117–133. [PubMed: 8115398]

26. O'Doherty A, et al. An aneuploid mouse strain carrying human chromosome 21 with Down syndrome phenotypes. Science. 2005; 309:2033–2037. [PubMed: 16179473]

27. Ghai R, et al. Phox homology band 4.1/ezrin/radixin/moesin-like proteins function as molecular scaffolds that interact with cargo receptors and Ras GTPases. Proc Natl Acad Sci U S A. 2011; 108:7763–7768. [PubMed: 21512128]

28. Wen L, et al. VPS35 haploinsufficiency increases Alzheimer's disease neuropathology. J Cell Biol. 2011; 195:765–779. [PubMed: 22105352]

29. Muhammad A, et al. Retromer deficiency observed in Alzheimer's disease causes hippocampal dysfunction, neurodegeneration, and Abeta accumulation. Proc Natl Acad Sci U S A. 2008; 105:7327–7332. [PubMed: 18480253]

30. Small SA. Retromer sorting: a pathogenic pathway in late-onset Alzheimer disease. Arch Neurol. 2008; 65:323–328. [PubMed: 18332244]

31. Small SA, et al. Model-guided microarray implicates the retromer complex in Alzheimer's disease. Ann Neurol. 2005; 58:909–919. [PubMed: 16315276]

32. Vilarino-Guell C, et al. VPS35 mutations in Parkinson disease. Am J Hum Genet. 2011; 89:162–167. [PubMed: 21763482]

33. Zimprich A, et al. A mutation in VPS35, encoding a subunit of the retromer complex, causes late-onset Parkinson disease. Am J Hum Genet. 2011; 89:168–175. [PubMed: 21763483]

34. Merhav M, et al. Behavioral interference and C/EBPbeta expression in the insular-cortex reveal a prolonged time period for taste memory consolidation. Learn Mem. 2006; 13:571–574. [PubMed: 16980548]

35. Milekic MH, Pollonini G, Alberini CM. Temporal requirement of C/EBPbeta in the amygdala following reactivation but not acquisition of inhibitory avoidance. Learn Mem. 2007; 14:504–511. [PubMed: 17644752]

36. Taubenfeld SM, Milekic MH, Monti B, Alberini CM. The consolidation of new but not reactivated memory requires hippocampal C/EBPbeta. Nat Neurosci. 2001; 4:813–818. [PubMed: 11477427]

37. Alberini CM, Ghirardi M, Metz R, Kandel ER. C/EBP is an immediate-early gene required for the consolidation of long-term facilitation in Aplysia. Cell. 1994; 76:1099–1114. [PubMed: 8137425]

38. Cramer NP, Best TK, Stoffel M, Siarey RJ, Galdzicki Z. GABAB-GIRK2-mediated signaling in Down syndrome. Adv Pharmacol. 2010; 58:397–426. [PubMed: 20655490]

39. Best TK, Siarey RJ, Galdzicki Z. Ts65Dn, a mouse model of Down syndrome, exhibits increased GABAB-induced potassium current. Journal of neurophysiology. 2007; 97:892–900. [PubMed: 17093127]

40. Balana B, et al. Mechanism underlying selective regulation of G protein-gated inwardly rectifying potassium channels by the psychostimulant-sensitive sorting nexin 27. Proc Natl Acad Sci U S A. 2011; 108:5831–5836. [PubMed: 21422294]

41. Gomis RR, Alarcon C, Nadal C, Van Poznak C, Massague J. C/EBPbeta at the core of the TGFbeta cytostatic response and its evasion in metastatic breast cancer cells. Cancer Cell. 2006; 10:203–214. [PubMed: 16959612]

42. Sterneck E, Tessarollo L, Johnson PF. An essential role for C/EBPbeta in female reproduction. Genes Dev. 1997; 11:2153–2162. [PubMed: 9303532]

43. Qiu Z, Ghosh A. A calcium-dependent switch in a CREST-BRG1 complex regulates activity-dependent gene expression. Neuron. 2008; 60:775–787. [PubMed: 19081374]

44. Liu Y, et al. Intracellular trafficking of presenilin 1 is regulated by beta-amyloid precursor protein and phospholipase D1. The Journal of biological chemistry. 2009; 284:12145–12152. [PubMed: 19276086]

45. Ehlers MD. Reinsertion or degradation of AMPA receptors determined by activity-dependent endocytic sorting. Neuron. 2000; 28:511–525. [PubMed: 11144360]
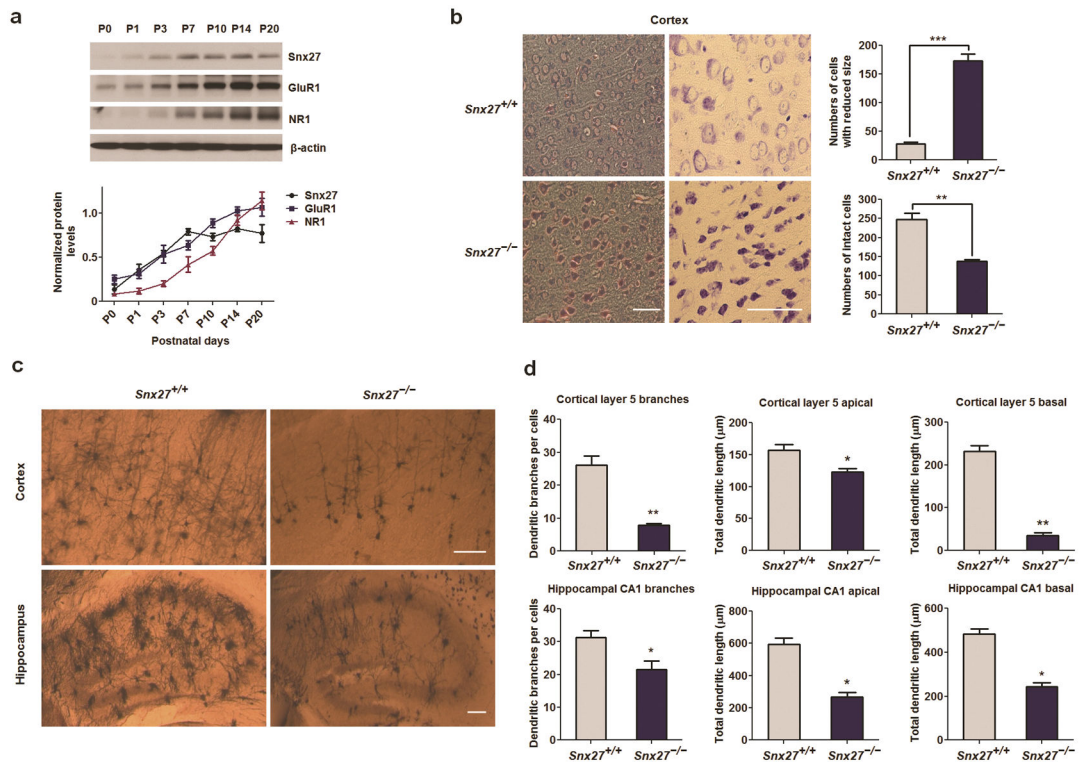
**Figure 1. Neuropathology in the cortex and hippocampus of *Snx27*<sup>−/−</sup> mice**

(**a**) Expression pattern of Snx27, GluR1 and NR1 in the developmental mouse cerebrum. Brain lysates of C57Bl/6 mice at different postnatal days were analyzed by western blot to detect Snx27, GluR1, NR1 and β-actin (as loading control). Data represent mean ± s.e.m., *n* = 3.

(**b**) Decreased number and size of neurons in the cortex of *Snx27*<sup>−/−</sup> mice. Low (left panels) and high (right panels) magnification views of Nissl staining sections from *Snx27*<sup>+/+</sup> (top panels) and *Snx27*<sup>−/−</sup> (bottom panels) mice (P14). Data represent mean ± s.e.m., *n* = 4. *P* values were calculated using two-tailed Student's t test, *$P < 0.05$, **$P < 0.01$, ***$P < 0.001$. Bar=50μm.

(**c,d**) Decreased dendritic branches and lengths in cerebral cortex and hippocampus in *Snx27*<sup>−/−</sup> mice. Golgi staining of cortex (upper panels) and hippocampus (lower panels) of *Snx27*<sup>+/+</sup> (left panels) and *Snx27*<sup>−/−</sup> (right panels) mice (P14) are presented in (**c**). Quantitative analysis of apical and basal dendrites and total branch points in cortical layer 5 pyramidal and hippocampal neurons in *Snx27*<sup>+/+</sup> and *Snx27*<sup>−/−</sup> mice are shown in (**d**). Data represent mean ± s.e.m., *n* = 4. *P* values were calculated using two-tailed Student's t test, *$P < 0.05$, **$P < 0.01$, ***$P < 0.001$. Bar=100μm.
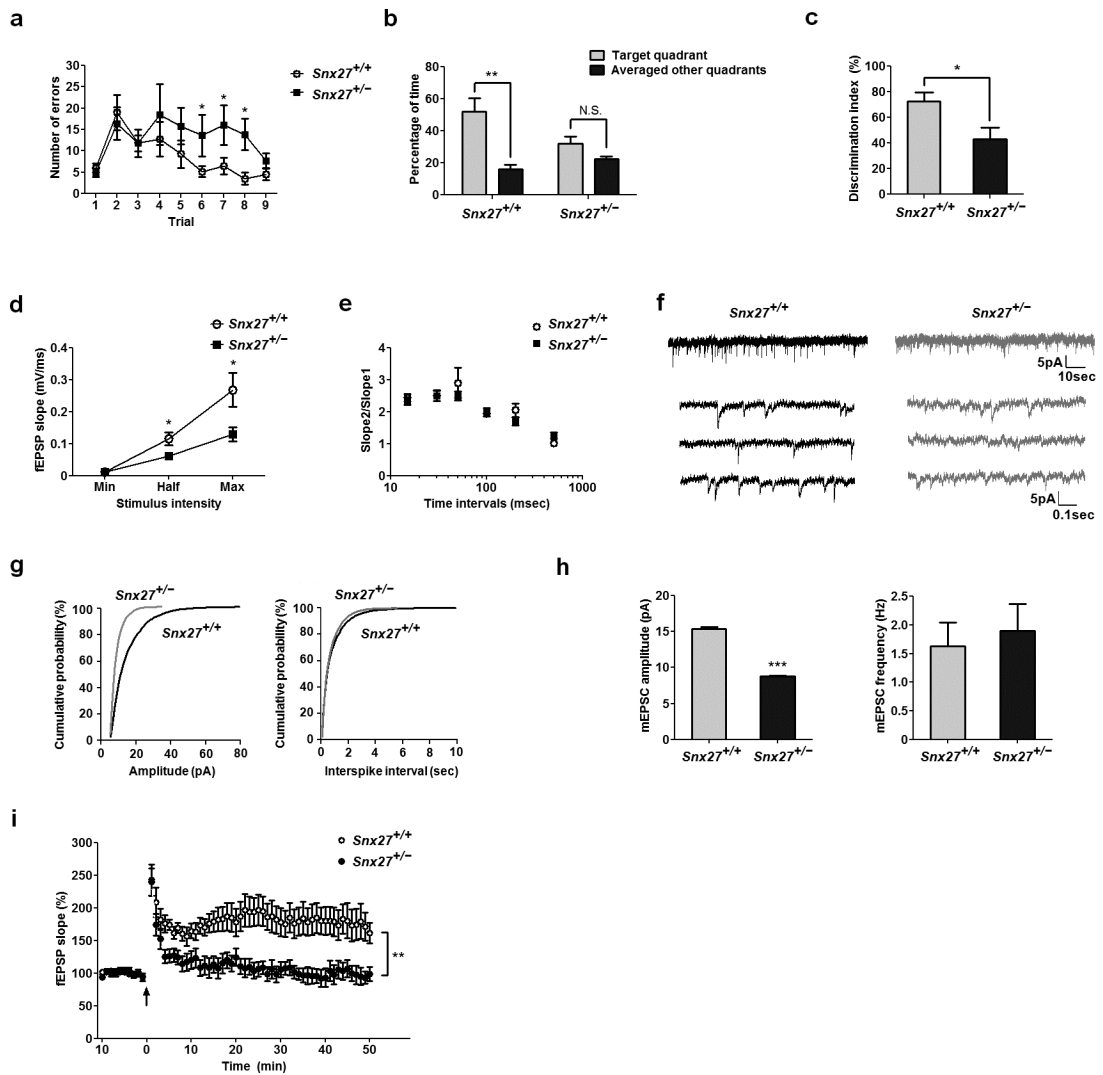
**Figure 2. Cognitive and synaptic deficits in *Snx27*^{+/−} mice**

(**a**) Barnes maze test for error counts in finding the escape chamber. Data represent mean ± s.e.m., *n* = 10. *P* values were calculated using repeated-measures ANOVA, *$P < 0.05$.

(**b**) Barnes maze probe test. Data represent mean ± s.e.m., *n* = 10. *P* values were calculated using nonparametric t test, **$P < 0.01$.

(**c**) Novel object recognition test. Data represent mean ± s.e.m., *n* = 10. *P* values were calculated using nonparametric t test, *$P < 0.05$.

(**d**) Input-output curves for basal synaptic transmission in hippocampal slices from *Snx27*^{+/+} (*n* = 4) and *Snx27*^{+/−} (*n* = 8) mice. Data represent mean ± s.e.m. *P* values were calculated using two-tailed Student's t test, *$P < 0.05$.

(**e**) Paired-pulse facilitation (PPF) in *Snx27*^{+/+} (*n* = 6) and *Snx27*^{+/−} (*n* = 8) hippocampal neurons. Data represent mean ± s.e.m. *P* values were calculated using two-tailed Student's t test, $P > 0.05$.

(**f**) Representative mEPSC recordings in CA1 neurons from hippocampal slices of *Snx27*^{+/+} and *Snx27*^{+/−} mice at 1-month of age.

(**g**) Cumulative probability distributions of mEPSC amplitude and frequency for $Snx27^{+/+}$ ($n$ = 8) and $Snx27^{+/-}$ ($n$ = 9) mice.

(**h**) Mean mEPSC amplitude and frequency in $Snx27^{+/+}$ ($n$ = 8) and $Snx27^{+/-}$ ($n$ = 9) neurons. Data represent mean ± s.e.m. $P$ values were calculated using two-tailed Student's t test, ***$P < 0.001$.

(**i**) CA1 LTP in $Snx27^{+/+}$ and $Snx27^{+/-}$ mouse hippocampal slices. Data represent mean ± s.e.m. $P$ values were calculated using repeated-measures ANOVA on the last 10 min of data, **$P < 0.01$.
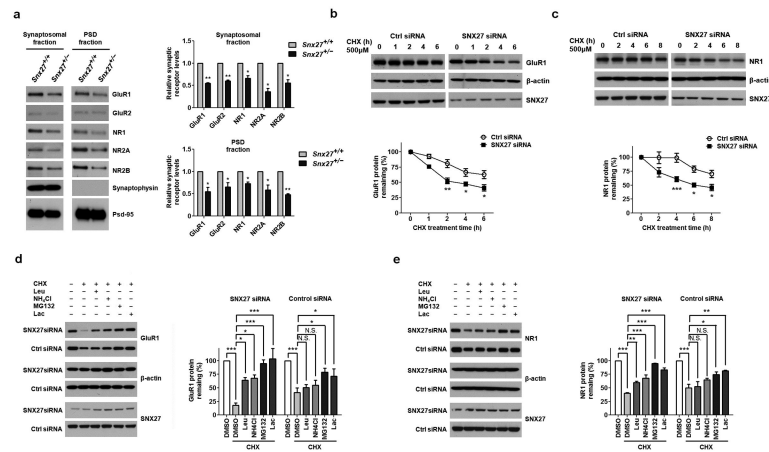
**Figure 3. Down-regulation of SNX27 affects stability of NMDARs and AMPARs**

(**a**) Protein levels of glutamate receptor subunits GluR1, GluR2, NR1, NR2A and NR2B in synaptosomal and PSD fractions derived from $Snx27^{+/+}$ and $Snx27^{+/−}$ mice. Data represent mean ± s.e.m., $n = 3$. $P$ values were calculated using two-tailed Student's t test, $*P < 0.05$, $**P < 0.01$.

(**b,c**) Time course of GluR1 degradation upon SNX27 knockdown in GluR1-HEK293 or NR1-HEK293 cells. Western blot analyses of GluR1 (**b**) or NR1 (**c**) and β-actin were performed after cycloheximide (CHX, 500 μM) treatment for indicated time periods. Signal intensity for GluR1 and NR1 was standardized to the signal intensity of β-actin and normalized to 100% at time 0. Data represent mean ± s.e.m., $n = 3$. $P$ values were calculated using repeated-measures ANOVA, $*P < 0.05$, $**P < 0.01$, $***P < 0.001$.

(**d,e**) Rescued degradation of GluR1 (**d**) and NR1 (**e**) by lysosomal and proteasomal inhibitors in GluR1-HEK293 or NR1-HEK293 cells with SNX27 siRNA and control siRNA. Cells were treated with CHX (500 μM) for 8h, in the presence of DMSO (−), lysosomal inhibitors (100 μg ml$^{−1}$ leupeptin (Leu); 200 μM chloroquine (CLQ)), or proteasomal inhibitors (10 μM lactacystin (Lac), or 10 μM MG132), as indicated. Data represent mean ± s.e.m., $n = 3$. $P$ values were calculated using one-way ANOVA, $*P < 0.05$, $**P < 0.01$, $***P < 0.001$.
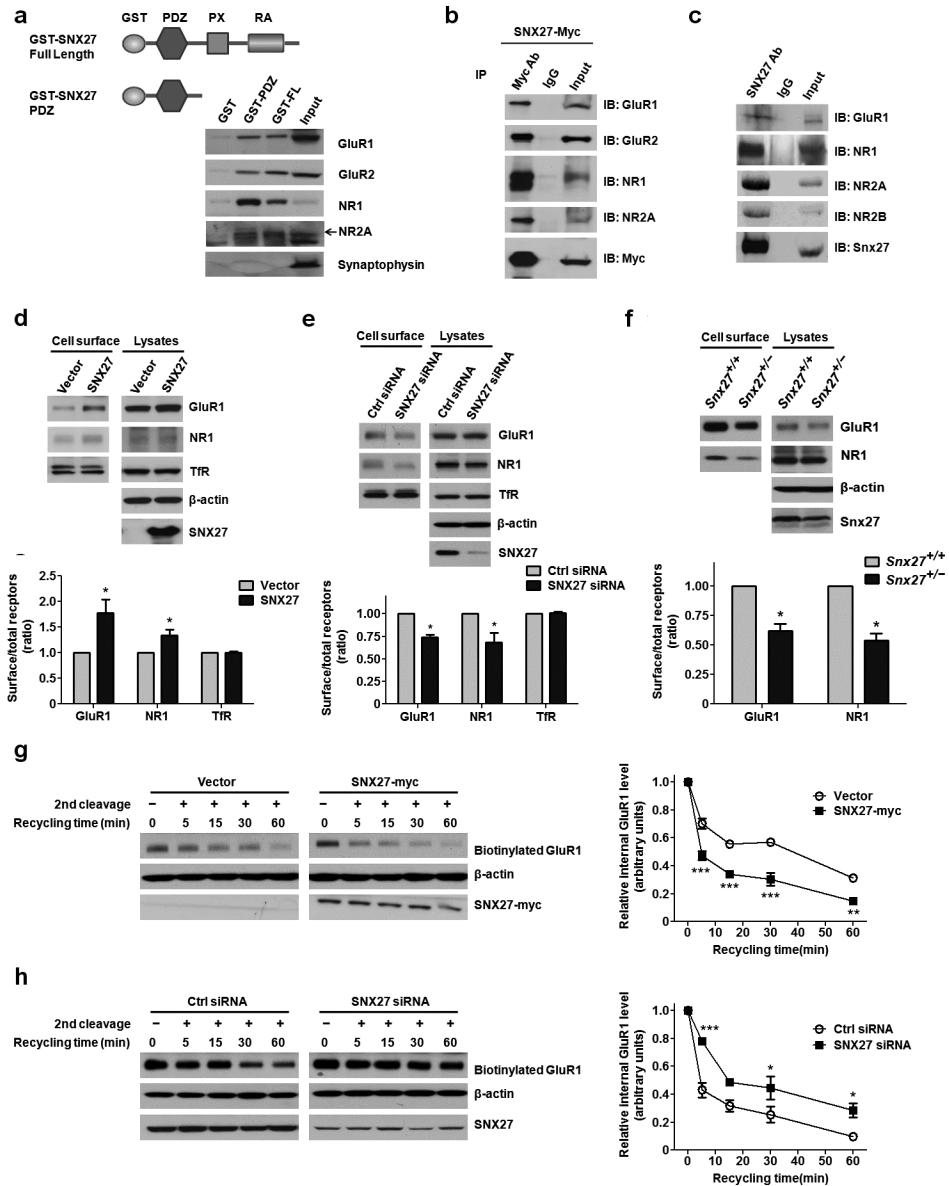
**Figure 4. SNX27 interacts with glutamate receptors and regulates recycling to the cell surface**

(**a**) Pull-down of glutamate receptors by recombinant GST-SNX27 Full-length (SNX27 FL) or GST-SNX27 PDZ domain.

(**b**) Co-immunoprecipitation between exogenously expressed myc-SNX27 and glutamate receptors.

(**c**) Co-Immunoprecipitation between endogenous Snx27 and endogenous glutamate receptors in C57Bl/6 mice brains.

(**d**) Cell surface expression of GluR1 or NR1 in the GluR1-HEK293 or NR1-HEK293 cells upon SNX27 over-expression, as seen by a surface biotinylation assay. Data represent mean ± s.e.m., $n = 3$. $P$ values were calculated using two-tailed Student's t test, *$P < 0.05$.

(**e**) Cell surface expression of GluR1 and NR1 in GluR1-HEK293 or NR1-HEK293 cells with SNX27 siRNA or control siRNA, as seen by a surface biotinylation assay. Data

represent mean ± s.e.m., $n = 3$. $P$ values were calculated using two-tailed Student's t test, *$P$ < 0.05.

(**f**) Cell surface expression of GluR1 and NR1 in $Snx27^{+/+}$ and $Snx27^{+/-}$ hippocampal neurons. Data represent mean ± s.e.m., $n = 3$. $P$ values were calculated using two-tailed Student's t test, *$P$ < 0.05.

(**g**) Increased recycling of GluR1 to the cell surface from intracellular compartments in GluR1-HEK293 cells upon SNX27 over-expression. Data represent mean ± s.e.m., $n = 3$. $P$ values were calculated using repeated-measures ANOVA, **$P$ < 0.001, ***$P$ < 0.0001.

(**h**) Decreased recycling of GluR1 in GluR1-HEK293 cells with SNX27 siRNA or control siRNA. Data represent mean ± s.e.m., $n = 3$. $P$ values were calculated using repeated-measures ANOVA, *$P$ < 0.05, ***$P$ < 0.0001.
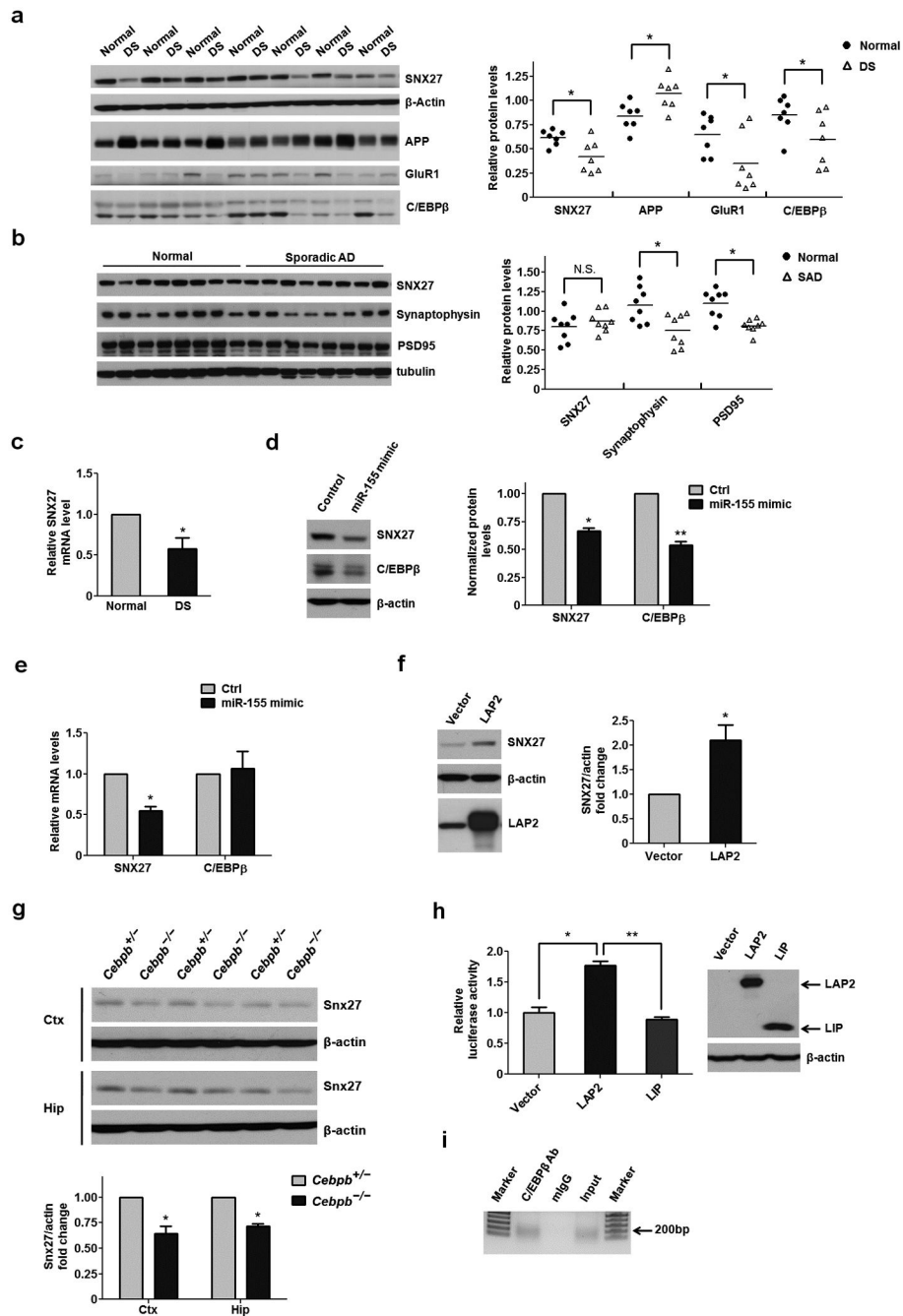
**Figure 5. Down-regulation of C/EBPβ via over-expression of miR-155 results in decreased SNX27 levels in Down syndrome brains**

(**a**) Western blot analysis of SNX27, C/EBPβ, APP and GluR1 in the cortex of age-matched controls (Normal) and Down syndrome individuals (DS). Signal intensity of the immunoblots was calculated and normalized to β-actin; $n = 7$. $P$ values were calculated using a nonparametric t test, *$P < 0.05$.

(**b**) Western blot analysis of SNX27 expression in the cortex of human with sporadic Alzheimer's disease and control brains. Signal intensity of the immunoblots was normalized to β-actin; $n = 8$. $P$ values were calculated using a nonparametric t test, $*P < 0.05$.

(**c**) Quantitative RT-PCR analyses of SNX27 mRNA levels in the cortex of Down syndrome individuals and normal controls. Data represent mean ± s.e.m., $n = 7$. $P$ values were calculated using a nonparametric t test, $*P < 0.05$.

(**d**) Western blot analyses of C/EBPβ and SNX27 protein levels in MC-IXC cells transfected with miR-155 or control mimic. Data represent mean ± s.e.m., $n = 3$. $P$ values were calculated using two-tailed Student's t test, $**P < 0.01$.

(**e**) Quantitative RT-PCR analyses of SNX27 and C/EBPβ mRNA levels in MC-IXC cells transfected with miR-155 or control mimic. Data represent mean ± s.e.m., $n = 3$. $P$ values were calculated using two-tailed Student's t test, $*P < 0.05$, $**P < 0.01$.

(**f**) Western blot analysis for SNX27 expression in MC-IXC cells transfected with LAP2 or control. Data represent mean ± s.e.m., $n = 3$. $P$ values were calculated using two-tailed Student's t test, $*P < 0.05$.

(**g**) Western blot analysis of Snx27 expression in the cortex and hippocampus from $Cebpb^{+/-}$ and $Cebpb^{-/-}$ mice. Data represent mean ± s.e.m., $n = 3$. $P$ values were calculated using two-tailed Student's t test, $*P < 0.05$.

(**h**) Firefly luciferase reporter assay for *SNX27* promoter activity. Data represent mean ± s.e.m., $n = 4$. $P$ values were calculated using two-tailed Student's t test, $*P < 0.05$.

(**i**) Binding of C/EBPβ to the *SNX27* promoter as determined by a Chromatin IP assay.
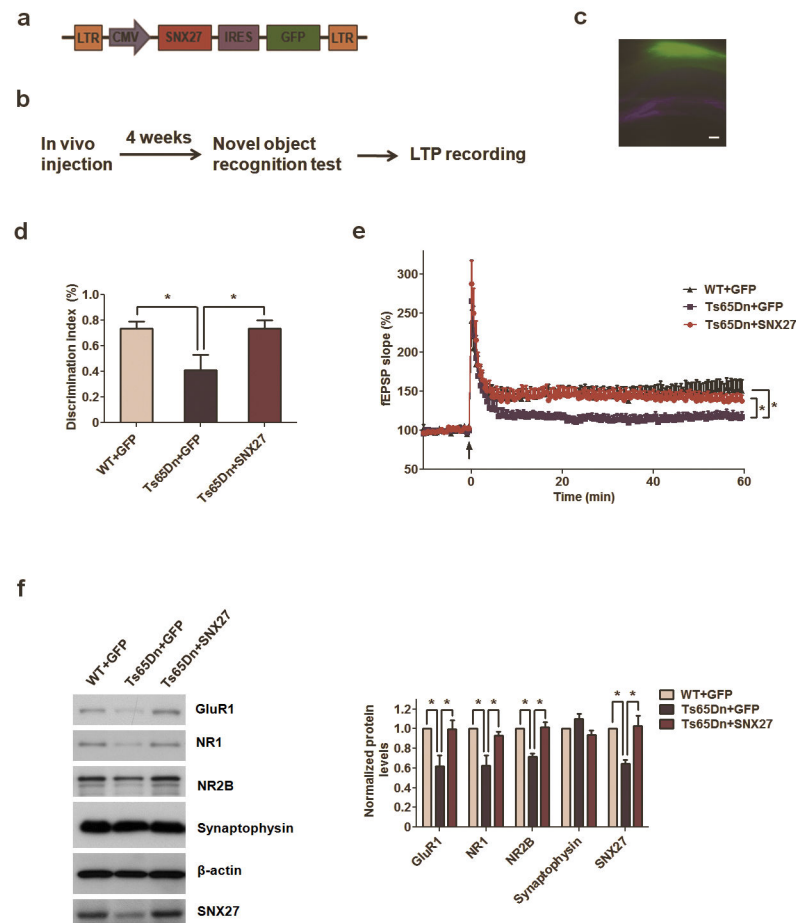
**Figure 6. SNX27 rescues cognitive and synaptic deficits in Ts65Dn mice**

(**a**) Schematic illustration of Adeno-associated virus (AAV) construct of human SNX27 with IRES-GFP.

(**b**) Workflow of stereotactic AAV injection rescue experiments.

(**c**) AAV-SNX27 GFP fluorescence in hippocampus showing infected region of mouse brain. Bar=200μm.

(**d**) Hippocampal injection of AAV-SNX27 rescued cognitive deficits of 7~8 months old Ts65Dn mice in novel object recognition test. Data represent mean ± s.e.m., WT+GFP ($n =$ 8), Ts65Dn+GFP ($n = 5$), Ts65Dn+SNX27 ($n = 7$). $P$ values were calculated using one-way ANOVA, *$P$ <0.05.

(**e**) Hippocampal injection of AAV-SNX27 rescued CA1 LTP deficits of 7~8 months old Ts65Dn mice. Data represent mean ± s.e.m., WT+GFP ($n = 7$ slices), Ts65Dn+GFP ($n = 9$ slices), Ts65Dn+SNX27 ($n = 10$ slices). $P$ values were calculated using repeated-measures ANOVA on the last 10 min of data, *$P$ <0.05.

(**f**) Western blot analysis of GluR1, NR1, NR2B and other synaptic proteins after intrahippocampal AAV-SNX27 or AAV-GFP injection into Ts65Dn mice. Data represent mean ± s.e.m., $n = 3$. $P$ values were calculated using one-way ANOVA, *$P < 0.05$.